Digital self-interference cancellation in inter-band carrier aggregation transceivers: Algorithm and digital implementation perspectives

Digital Self-interference Cancellation in Inter-band Carrier Aggregation Transceivers: Algorithm and Digital Implementation Perspectives

Muhammad Zeeshan Waheed, Dani Korpi, Adnan Kiayani, Lauri Anttila, and Mikko Valkama

Laboratory of Electronics and Communications Engineering, Tampere University of Technology, Finland
e-mail: muhammad.waheed@tut.fi

***Abstract*—In this paper we study and analyze the problem of self-interference in transceivers performing inter-band carrier aggregation, where separate power amplifiers (PAs) are used for each component carrier (CC). The self-interference stems from the nonlinear behaviour of the passive RF components at the transmitter, which results in passive intermodulation terms that in some cases fall onto the RX band. Moreover, also the individual PAs distort the CCs in a nonlinear fashion, which means that the self-interference is in fact produced by a cascade of two nonlinearities. This is something that has largely been ignored in earlier literature. Hence, in this work, a signal model is derived that considers both the nonlinearity of the PAs and the passive components, resulting in a highly efficient digital cancellation solution. Using realistic waveform simulations, it is shown to outperform the existing digital cancellers that neglect the PA-induced nonlinear distortion. Also the computational complexity of the proposed digital canceller is analyzed in detail. All in all, the findings indicate that the developed digital cancellation solution is a feasible option for improving the receiver sensitivity of mobile devices utilizing inter-band carrier aggregation.**

I. Introduction

The continuously increasing user demands for high data throughput in wireless systems can be satisfied by utilizing wider transmission bandwidths. Therefore, modern cellular handsets need to support a wide range of frequency bands, and some of them simultaneously, so that a large aggregated bandwidth can be realized. However, due to current allocation and licensing of the radio spectrum, allocating a continuous spectrum to a single user is practically impossible. To alleviate this issue, the carrier aggregation (CA) technique introduced in LTE-Advanced enables flexible expansion of the transmission bandwidth by aggregating spectrum resources either from the same LTE frequency band (intra-band) or from different frequency bands (inter-band CA) [1]–[3]. With inter-band CA, multiple transmissions can occur simultaneously over different LTE bands, where each contiguous transmit signal is referred to as component carrier (CC), and it greatly enhances the flexibility and efficiency of the radio spectrum usage.

In general, noncontiguous transmission poses a variety of practical implementation related challenges for the radio transceivers [3], [4]. More specifically, when a noncontiguous signal propagates through a nonlinear radio frequency (RF) front-end component, unwanted intermodulation distortion (IMD) products are produced. These IMD products lie at specific intermodulation (IM) sub-bands which are integer linear combinations of the CC center-frequencies [4]. In some cases, some of the IM sub-bands can appear in the own receiver (RX) operating band, causing self-interference. This has recently been acknowledged in 3GPP for various band combinations in inter-band CA [5], [6].

A dominant source of nonlinear distortion in radio transceivers is the transmitter (TX) power amplifier (PA). However, with inter-band CA transmissions where each CC is typically amplified by a separate PA [3], [7], spurious signals generated by the passive RF front-end components can also be significant and, in turn, may cause self-interference to the RX. In recent years, several digital cancellation techniques have been proposed that target to suppress the PA nonlinearity induced self-interference [4]–[9]. On the other hand, the works in [10]–[12] consider only the digital cancellation of passive IMD, while neglecting the nonlinear distortion in the individual TX PAs. In this paper, we develop a complete behavioral model incorporating the joint effects of the cascaded nonlinearities of the PA and the passive components. Then, building on this model, we develop a digital cancellation technique to jointly mitigate the self-interference caused by the nonlinearity of the TX PAs and the passive components in the receiver digital baseband. Waveform simulation results show that the proposed digital cancellation scheme provides substantial self-interference suppression, thus reducing the RF components' linearity requirements, cost, and complexity.

The rest of the paper is organized as follows. In the following section, we discuss the implementation challenges of a radio transceiver supporting inter-band CA. In Section III, essential signal models related to the cascaded nonlinearity of the TX PAs and the passive components are presented, together with the proposed digital cancellation technique. The performance evaluation of the proposed technique with full waveform simulations is reported in Section IV, and conclusions are made in Section V.

II. Inter-band Carrier Aggregation with Non-ideal RF Components

Inter-band CA allows combining the spectrum resources from different LTE operating bands in order to provide increased data rate. It can be divided into CA among the low-

978-1-5386-0446-5/17/$31.00

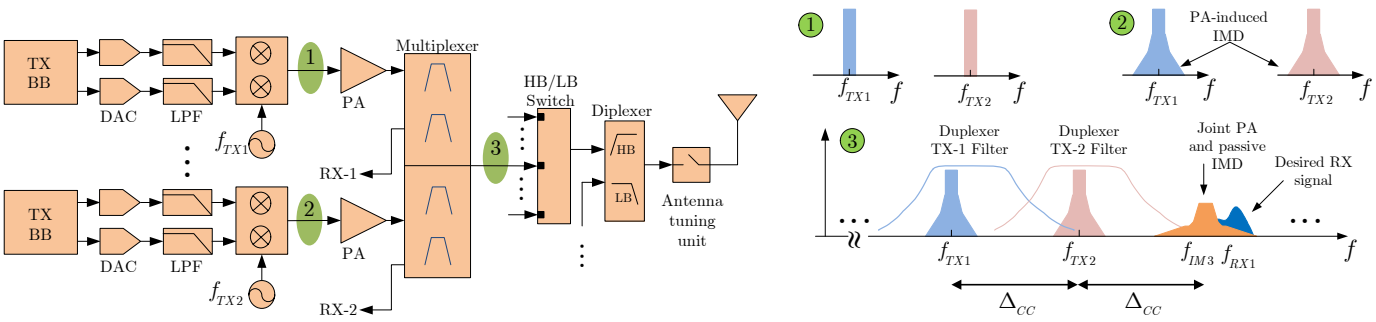

Fig. 1: (a) Block diagram of the considered transmitter architecture for inter-band CA FDD transceiver, and (b) a spectral illustration of the unwanted IMD products created due to the nonlinearity of the TX PAs and the passive components, appearing in one of the configured RX operating bands.

band ($<$ 1 GHz) carriers and high-band ($>$ 1 GHz) carriers (LB-HB CA) where the CC center-frequencies are further apart, or CA of similar frequencies, i.e., LB-LB CA or HB-HB CA [13]. In this paper, we consider the inter-band CA of similar frequencies, such as CA of LTE Band 1 and Band 3 (CA B1+3), CA B5+13, or CA B4+8, among others. The considered radio architecture, shown in Fig. 1(a), is comprised of separate TX and RX chains for each aggregated LTE band which, in general, is a feasible candidate TX architecture to support a wide range of LTE bands [7]. Each CC is amplified by a separate PA, and different LTE bands are combined using a multiplexer. The radio transceivers of different LTE bands share the same antenna and thereby a band selection switch and a diplexer are also employed.

As discussed earlier, the nonlinear behavior of the RF components in the radio transceiver and RF front-end creates unwanted IMD products. The IMD products created due to the PA nonlinearity appear as spectral regrowth around the transmit CCs, whereas the passive front-end components, such as the multiplexer, the switch, and the diplexer, create IMD products of the CCs which appear at various different center-frequencies. In general, the IM frequencies are linear combinations of the CC center-frequencies, with certain integer coefficients. In some CA band combinations, the center-frequencies of these IMD products can coincide with one of the configured RX frequencies and may lead to RX desensitization, as shown in Fig. 1(b). For example, if we consider the CA of B1+B3 and assume that the center frequency of CC1 is $f_{\mathrm{TX1}} = 1950$ MHz and the center frequency of CC2 is $f_{\mathrm{TX2}} = 1760$ MHz, then the third-order IM sub-band, located at $f = 2f_{\mathrm{TX1}} - f_{\mathrm{TX2}} = 2140$ MHz, falls within the RX band of B1. Other similar band combination examples may include, e.g., CA B3+8, B2+4, B5+7, etc. The relative powers of the IMD components depend on the PA and the passive components' linearity characteristics, and can be very strong even with state-of-the-art RF components.

To prevent the RX desensitization in inter-band CA transceivers, one could consider either reducing the transmit power or alternatively relaxing the receiver reference sensitivity requirements, known as maximum power reduction (MPR) and maximum sensitivity degradation (MSD) in the context of LTE-Advanced, respectively [5], [14]. The former decreases the relative strength of the IMD, while the latter simply takes the IMD-induced interference into account in the link budget calculations. However, such methods will severely compromise the uplink coverage, and consequently a more convenient option might be to just improve the quality of the RF components at the expense of increased overall cost.

Motivated by previous discussion and keeping in view the drawbacks of the above discussed solutions, in this paper we develop an advanced digital self-interference cancellation solution for inter-band CA radio transceivers. This means that the self-interference can be dealt with without any decrease in the uplink coverage, or without significant increase in the overall cost of the transceiver.

III. Passive Intermodulation Modeling and Proposed Digital Cancellation

As already discussed, in this paper we consider a scenario where two UL CCs, transmitted within an LTE mobile device, produce IMD onto the DL frequency band. In particular, assuming that the UL transmission occurs on LTE UL bands 1 and 3, one of the 3rd-order IMD products will fall directly onto the LTE DL Band 1. Note that there are also band combinations that can produce harmful IMD of different orders, but in this work the emphasis is only on this band combination and the 3rd-order IMD that is being produced by the passive components.

A. Self-interference Model and Canceller Structure

In general, denoting the baseband UL signals on Bands 1 and 3 by $s_1(n)$ and $s_3(n)$, respectively, and considering only the 3rd-order passive intermodulation (PIM), we can express the PIM product at RF as

$$s_{\mathrm{PIM}}(n) = \alpha_{\mathrm{PIM}} \left(\alpha_1 \,\mathrm{Re}\left\{s_1(n)e^{j\omega_1 n}\right\} + \alpha_2 \,\mathrm{Re}\left\{s_3(n)e^{j\omega_3 n}\right\}\right)^3 \quad (1)$$

where ω_1 is the center-frequency of the CC on Band 1, ω_3 is the center-frequency of the CC on Band 3, and α_X are unknown coefficients. It is then easy to show by expanding (1)

that the baseband-equivalent self-interference signal falling onto the RX band is as follows:

$$s_{\mathrm{PIM}}^{\mathrm{RX}}(n) = \alpha_{\mathrm{PIM}}^{\mathrm{RX}} s_1(n)^2 s_3^*(n), \tag{2}$$

where we have reverted to baseband-equivalent notation for notational simplicity, the zero frequency corresponding to $2\omega_1 - \omega_3$. Note that (1) generates also several other nonlinear terms but none of them fall near the considered RX band and can consequently be ignored in this analysis.

It is important to note that also the PAs themselves produce some nonlinear distortion, which should be modeled, in addition to PIM. Having also a 3rd-order model for both PAs, we can write

$$s_1(n) = \alpha_{11} x_1(n) + \alpha_{13} x_1(n)^2 x_1^*(n) \tag{3}$$

$$s_3(n) = \alpha_{21} x_3(n) + \alpha_{23} x_3(n)^2 x_3^*(n) \tag{4}$$

where $x_1(n)$ and $x_3(n)$ are the original TX data signals for the two PAs on LTE UL Bands 1 and 3, respectively, and α_{xy} are the coefficients for the PA models. Substituting then (3) and (4) into (2), the final baseband equivalent self-interference signal can be written as

$$\begin{aligned} s_{\mathrm{PIM}}^{\mathrm{RX}}(n) = {} & \alpha_1 x_1(n)^2 x_3^*(n) + \alpha_2 x_1(n)^3 x_1^*(n) x_3^*(n) \\ & + \alpha_3 x_1(n)^4 x_1^*(n)^2 x_3^*(n) + \alpha_4 x_1(n)^2 x_3^*(n)^2 x_3(n) \\ & + \alpha_5 x_1(n)^3 x_1^*(n) x_3^*(n)^2 x_3(n) \\ & + \alpha_6 x_1(n)^4 x_1^*(n)^2 x_3^*(n)^2 x_3(n) \end{aligned} \tag{5}$$

Hence, the final signal model consists of six basis functions, whose coefficients (α_1–α_6) must be estimated in order to regenerate and cancel the PIM-induced self-interference in the receiver.

It should also be noted that the first basis function ($x_1(n)^2 x_3^*(n)$) corresponds to a model with linear PAs, and it can consequently be considered as a benchmark for the proposed digital canceller, which also incorporates the nonlinearity of the PAs. Such a model has been proposed, for instance, in [10], albeit with memory. However, note that the first basis function is still the most dominant one in any practical system as the linear signal term is obviously stronger than any of the nonlinearities.

B. Parameter Estimation

Noting that (5) is in fact a linear-in-parameters model, the parameter estimation can be carried out with linear least squares (LS). For this, let us denote the six basis functions in (5) as follows:

$$\begin{aligned} \phi_1(n) &= x_1(n)^2 x_3^*(n) \\ \phi_2(n) &= x_1(n)^3 x_1^*(n) x_3^*(n) \\ \phi_3(n) &= x_1(n)^4 x_1^*(n)^2 x_3^*(n) \\ \phi_4(n) &= x_1(n)^2 x_3^*(n)^2 x_3(n) \\ \phi_5(n) &= x_1(n)^3 x_1^*(n) x_3^*(n)^2 x_3(n) \\ \phi_6(n) &= x_1(n)^4 x_1^*(n)^2 x_3^*(n)^2 x_3(n) \end{aligned} \tag{6}$$

Then, the data matrix for the nth time instant is as follows:

$$\begin{aligned} & \boldsymbol{\Phi}(n) \\ & = \begin{bmatrix} \phi_1(n-N+1) & \phi_2(n-N+1) & \cdots & \phi_6(n-N+1) \\ \phi_1(n-N+2) & \phi_2(n-N+2) & \cdots & \phi_6(n-N+2) \\ \vdots & \vdots & \ddots & \vdots \\ \phi_1(n) & \phi_2(n) & \cdots & \phi_6(n) \end{bmatrix} \end{aligned} \tag{7}$$

where N is the number of samples used for estimation. The parameter estimate is then simply calculated as

$$\widehat{\boldsymbol{\alpha}} = \left(\boldsymbol{\Phi}^H(n)\boldsymbol{\Phi}(n)\right)^{-1} \boldsymbol{\Phi}^H(n)\boldsymbol{y} \tag{8}$$

where $\hat{\boldsymbol{\alpha}} = \begin{bmatrix} \widehat{\alpha}_1 & \widehat{\alpha}_2 & \cdots & \widehat{\alpha}_6 \end{bmatrix}^T$ contains the estimate for each coefficient, and $\boldsymbol{y}$ is the received signal before any cancellation. Moreover, $(\cdot)^H$ denotes the Hermitian transpose, while $(\cdot)^T$ denotes the regular transpose. The actual cancellation performance can then be evaluated by regenerating the self-interference over another observation period, using the estimated coefficients. The signal after the cancellation can be written as follows:

$$y_{\mathrm{c}}(n) = y(n) - \sum_{i=1}^{6} \widehat{\alpha}_i \phi_i(n), \tag{9}$$

where $y(n)$ is the nth sample of the overall received signal before any cancellation. In the forthcoming results section, the performance of the proposed scheme is compared to the case where linear PAs are assumed, which means that only the first basis function is included in the cancellation processing, as discussed earlier. This is essentially a memoryless version of the digital cancellation solution presented in [10].

C. Computational Complexity of the Cancellation Procedure

Let us then briefly analyze the computational complexity of the proposed digital cancellation solution. The overall cancellation procedure involves in principle two steps, which are as follows:

- Estimating the coefficients with LS
- Regenerating and canceling the self-interference signal

However, considering that the nonlinear behaviour of the PAs and the passive components can be expected to be largely time-invariant, the estimation stage is performed only relatively infrequently. Hence, the overall computational complexity of the digital canceller is mainly determined by the second stage, as it is being performed constantly. For this reason, it is sufficient to consider only the second stage in this analysis.

It can easily be observed from (6) that generating the six basis function samples for one time instant requires 36 complex multiplications. Furthermore, generating the cancellation signal itself, as shown in (9), requires 6 complex multiplications and 5 complex additions per one time instant. Taking into account also the actual cancellation where the regenerated self-interference signal is subtracted from the received signal, the total number of required computations per each received sample is ***42 complex multiplications and 6 complex additions***.

If some latency in generating the basis functions is acceptable, the number of multiplications can be decreased by presenting the basis functions in a recursive form as follows:

$$\begin{aligned}\phi_1(n) &= x_1(n)^2 x_3^*(n)\\ \phi_2(n) &= \phi_1(n)x_1(n)x_1^*(n)\\ \phi_3(n) &= \phi_2(n)x_1(n)x_1^*(n)\\ \phi_4(n) &= \phi_1(n)x_3(n)x_3^*(n)\\ \phi_5(n) &= \phi_4(n)x_1(n)x_1^*(n)\\ \phi_6(n) &= \phi_5(n)x_1(n)x_1^*(n)\end{aligned} \tag{10}$$

In this case, it can be calculated from (10) that generating the six basis functions for one time instant requires only 10 complex multiplications. Taking into account also the computations involved in generating the cancellation signal and performing the subtraction, in total ***16 complex multiplications and 6 complex additions*** are needed in this case for each received sample. However, as mentioned, the cost of this decreased computational complexity is the increased latency in generating the basis functions. It should also be mentioned that it might be possible to further reduce the number of multiplications by using alternative representations of the TX signals, although these aspects are out of the scope of this paper.

IV. Simulation Results

A. Simulator Description

The proposed digital cancellation solution is then evaluated using a waveform simulator implemented with Matlab, which is modeling the transceiver illustrated in Fig. 1. The two CCs are transmitted on LTE UL bands 1 and 3, as per the earlier discussions, the transmit waveforms being LTE UL signals. Furthermore, realistic baseband-equivalent models for the different components are also included in the simulator. Firstly, the model for each PA is extracted by measuring the characteristics of an actual real-life PA under the utilized transmit power. The memory effects of the PA are also included in the modeling. The frequency selective behaviour of the duplexer/multiplexer is also considered in the simulator, although results are also provided for a frequency-flat ideal duplexer for reference. The IMD is then produced within the simulator by feeding the sum transmit signal, consisting of two CCs, into a nonlinear model of an RF switch. This produces the PIM component that is falling onto the RX band. The relevant parameters used in the simulations are listed in Table I.

B. Cancellation Performance

The cancellation performance is first measured for a frequency-flat duplexer response. This means that the only memory within the system is that of the PAs. Figure 2 shows the spectra of observed self-interference signal, alongside with the signal spectra after the two different digital cancellers. The cancellation performance of the benchmark scheme with linear PA models, taken from [10], is clearly insufficient for such a weak received signal of interest, as the signal-to-interference-plus-noise ratio (SINR) is in this case negative. On the other hand, when utilizing all the six basis functions, i.e., modeling also the nonlinearity of the PAs, the self-interference can be cancelled almost 10 dB below the noise

TABLE I: The essential simulation parameters.

Parameter	Value
Bandwidth of the CCs	5 MHz
Total transmit power	23 dBm
Center frequencies of CCs	1760/1950 MHz
RX frequency	2140 MHz
IIP3 of the RF switch	70 dBm
Power of the RX signal	-91.5 dBm
Number of samples used for estimation (N)	10 000

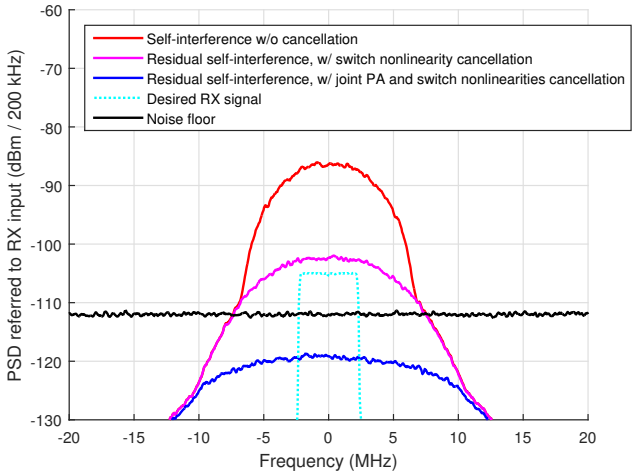

Fig. 2: The spectra of the observed PIM and the residual signals after cancellation. The received signal of interest is also shown for reference. Frequency-flat duplexer response.

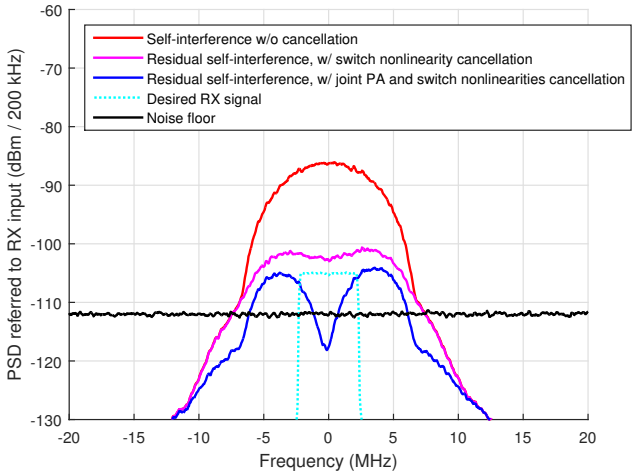

Fig. 3: The spectra of the observed PIM and the residual signals after cancellation. The received signal of interest is also shown for reference. Frequency-selective duplexer response.

floor. This means that the decrease in the SINR is less than half a decibel. Hence, the proposed canceller, with realistic nonlinearity models for the PAs and the passive components, is indeed capable of sufficient cancellation accuracy. Note that the parameter estimation within the simulator is performed using the total received signal that contains also the noise and the desired signal, although each signal component is shown separately in Fig. 2 for a better illustration.

Considering then a more challenging scenario where the duplexer has a frequency-selective response, Fig. 3 shows again the spectra of the different signal components. As can be observed, now the residual self-interference power is much higher also after the proposed canceller with PA nonlinearity modeling. This stems from the fact that the utilized signal model does not have any memory, and consequently it is not capable of modeling any frequency selectivity. This is not an issue when only the PAs have memory, as the resulting frequency selectivity is rather mild in nature. However, the frequency selectivity of the duplexer response is much more severe, and thereby the accuracy of the memoryless model is somewhat reduced. Nevertheless, it still outperforms the benchmark scheme with linear PA models, although now the residual self-interference decreases the SINR with both cancellers.

All in all, these findings confirm the high performance of the proposed digital canceller, thereby indicating that the nonlinearity of the PAs must be modeled when canceling PIM-induced self-interference in the receiver. However, Fig. 3 also demonstrates that the digital canceller should incorporate some memory to fully suppress the self-interference under practical circumstances. This is an important future work item for us, together with performing actual RF measurement–based cancellation experiments.

V. Conclusion

In this paper, we proposed a novel digital cancellation solution for dealing with the self-interference produced in transceivers utilizing inter-band carrier aggregation. The self-interference stems from the nonlinearity of the passive components, as separate power amplifiers are used for each component carrier. However, the nonlinear behaviour of the power amplifiers still affects the self-interference waveform, and hence it is also considered in the proposed digital canceller. Using waveform simulations, the developed digital canceller is shown to outperform the existing solutions, which neglect the nonlinearity of the PAs. As a future work item, we plan to extend the signal model to cover also the various memory effects occurring in the transmitter, while also using actual measured data to evaluate the cancellation performance under real-life conditions.

Acknowledgment

This work was supported by the Academy of Finland (under the projects 304147 In-Band Full-Duplex Radio Technology: Realizing Next Generation Wireless Transmission, and 301820 Competitive Funding to Strengthen University Research Profiles), the Finnish Funding Agency for Innovation (Tekes, under the project 5G Transceivers for Base Stations and Mobile Devices (5G TRx)), Tampere University of Technology Graduate School, Nokia Networks, TDK-EPCOS, Pulse, Sasken, and Huawei Technologies, Finland

References

[1] "Further advancements for E-UTRA physical layer aspects," 3GPP, Tech. Rep. 36.814, Mar. 2010, version 9.0.0, Release 9.

[2] M. Iwamura, K. Etemad, M. H. Fong, and R. Nory, "Carrier aggregation framework in 3GPP LTE-Advanced," *IEEE Communications Magazine*, vol. 48, no. 8, pp. 60–67, Aug. 2010.

[3] C. S. Park, L. Sundström, A. Wallen, and A. Khayallah, "Carrier aggregation for LTE-Advanced: Design challenges of terminals," *IEEE Communications Magazine*, vol. 51, no. 12, pp. 76–84, Dec. 2013.

[4] A. Kiayani, M. Abdelaziz, L. Anttila, V. Lehtinen, and M. Valkama, "Digital mitigation of transmitter-induced receiver desensitization in carrier aggregation FDD transceivers," *IEEE Transactions on Microwave Theory and Techniques*, vol. 63, no. 11, pp. 3608–3623, Dec. 2015.

[5] "LTE; evolved universal terrestrial radio access (E-UTRA); user equipment (UE) radio transmission and reception (3GPP TS 36.101, version 14.1.0, release 14)," ETSI, Sophia Antipolis Cedex, France, Sep. 2016.

[6] "LTE-advanced dual uplink inter-band carrier aggregation (CA) (3GPP TS 36.860, version 13.0.0, release 13)," ETSI, Sophia Antipolis Cedex, France, Jan. 2016.

[7] "Feasibility study for further advancements for E-UTRA (LTE-Advanced)," 3GPP, Tech. Rep. 36.912, Mar. 2013, version 14.0.0, Release 14.

[8] "R4-141306, band 1 and band 3 UE considerations for CA," Qualcomm Incorporated, San Jose Del Cabo, Mexico, 2014.

[9] A. Kiayani, L. Anttila, and M. Valkama, "Digital suppression of power amplifier spurious emissions at receiver band in FDD transceivers," *IEEE Signal Processing Letters*, vol. 21, no. 1, pp. 69–73, Jan. 2014.

[10] H. T. Dabag, H. Gheidi, S. Farsi, P. S. Gudem, and P. M. Asbeck, "All-digital cancellation technique to mitigate receiver desensitization in uplink carrier aggregation in cellular handsets," *IEEE Transactions on Microwave Theory and Techniques*, vol. 61, no. 12, pp. 4754–4765, Dec. 2013.

[11] H. T. Dabag, H. Gheidi, P. S. Gudem, and P. M. Asbeck, "All-digital cancellation technique to mitigate self-jamming in uplink carrier aggregation in cellular handsets," in *Proc. IEEE MTT-S International Microwave Symposium Digest (MTT)*, 2013.

[12] H. Gheidi, H. T. Dabag, Y. Liu, P. M. Asbeck, and P. S. Gudem, "Digital cancellation technique to mitigate receiver desensitization in cellular handsets operating in carrier aggregation mode with multiple uplinks and multiple downlinks," in *Proc. IEEE Radio and Wireless Symposium (RWS)*, 2015.

[13] "Inter-band carrier aggregation (3GPP TS, 36.850, version 1.1.0, release 11)," ETSI, Sophia Antipolis Cedex, France, Jul. 2013.

[14] "Way forward for interband class A2," Nokia Corporation and AT&T, Jeju Island, Korea, 2012.